Proceedings of the 17th World Congress
The International Federation of Automatic Control
Seoul, Korea, July 6-11, 2008

Hydrodynamic parameter estimation of an open frame unmanned underwater vehicle

Juan Pablo Julca Avila [*,1] **Newton Maruyama** [*]
Julio Cezar Adamowski [*]

[*] *Department of Mechatronics Engineering, Polytechnic School at the University of Sao Paulo, Av. Prof. Mello Moraes 2231, CEP 05508-900 So Paulo, BRAZIL*

Abstract: A semi-autonomous unmanned underwater vehicle (UUV), named VSOR, is being developed at the Laboratory of Sensors and Actuators at the University of Sao Paulo. The vehicle has been designed to provide inspection and intervention capabilities in specific missions in deep water oil fields. This work presents a methodology to identify the drag coefficients and virtual mass/inertia of an open-frame underwater vehicle using the system identification approach. Trials with the vehicle in a test tank have been performed. Using the vehicle on-board sensor information, the methodology is based on the utilisation of an uncoupled 1-DOF (degree of freedom) dynamic system equation of an underwater vehicle and the application of the integral method, which is the classical least squares algorithm, applied to the integral form of the system dynamic equations. An assessment of the feasibility of the method is presented.

Keywords: Hydrodynamic parameter estimation, Unmanned Underwater vehicles.

1. INTRODUCTION

A semi-autonomous unmanned underwater vehicle (UUV) of type open-frame, named VSOR, is being developed at the Laboratory of Sensors Actuators at the University of Sao Paulo. The name VSOR is an acronym which stands for *Veículo Submarino Operado Remotamente*, or translated into English, *Remotely Operated Underwater Vehicle*. Despite of the use of the *Remotely Operated* term, the VSOR has been conceived as having semi-autonomous behaviour, i.e., the vehicle can be remotely operated but have an autonomous mode that can be used to approach the target. The vehicle has been initially conceived to provide inspection and intervention capabilities in specific missions in deep water oil fields.

Most open-frame underwater vehicles have the following characteristics: two symmetry planes, low operation velocities ($< 1m/s$), passively stable in roll and pitch angular motions, and creeping and uncoupled motions. For this type of underwater vehicle, the 6-DOF motion dynamic equations might be simplified. As a result, an approximate uncoupled scalar dynamic model is obtained which is sufficiently precise for control system design. This scalar dynamic equation have three hydrodynamic parameters which are considered to be independent of Reynolds number: quadratic and linear drag coefficients, and virtual mass/inertia.

The application of system identification techniques to UUV's is concerned with the estimation of hydrodynamic coefficients that characterize the vehicle dynamics, using the data collected from free running experimental trials. Since this dynamic equation of motion can be formulated as an equation which is linear in the vector of parameters, the least-squares (LS) algorithm is the commonly used estimation algorithm. Caccia et al. [2000] and Ridao et al. [2004] use the LS method based on the integral of the system dynamic equation. This identification technique is known as the integral method. The advantage of using the integral method is that eliminates the need for acceleration measurements. An on-line adaptive identification method that has been recently proposed (Smallwood and Whitcomb [2003]) does not also requires acceleration measurements but it is limited to scalar uncoupled models. One drawback of the adaptive method is that it possesses several gains that must be empirically tuned. Very few previous works have reported UUV's parameter identification studies. Caccia et al. [2000] and Smallwood and Whitcomb [2003] report experimental trials and parameter validation. In this work, the integral method is adopted for the identification of the VSOR yaw motion dynamic model. The experimental results of the parameter estimation are presented and discussed.

This paper is organized as follows. Next section summarises the mechanical design of the VSOR and its thruster system, including the presentation of modelling and identification of a thruster dynamic model. Then it follows with the presentation of the uncoupled, 1-DOF lumped parameter model. Next section presents the VSOR yaw controller design. Next, it is presented the chosen parameter identification algorithm, the integral method. The numerical results of the identification of the VSOR yaw dynamic is presented and an assessment of the quality of parameter estimates are realised by calculating the error between the results of system model simulation and logged experimental data. Discussions about the accuracy

[1] Supported by a scholarship (Process no. 03/12807-4) of the Fundacao de Amparo a Pesquisa do Estado de Sao Paulo (FAPESP), BRAZIL.

Fig. 1. Physical layout of the VSOR.

of parameter estimates and the choice of experimental input excitation signals are presented. And finally, some conclusions about the feasibility of the method are drawn.

2. THE VSOR DESIGN

2.1 Mechanical Design and Thrusters Configuration

The vehicle configuration is composed of an aluminum tubular structure, $l = 1.4m \times w = 1.2m \times h = 0.9m$, equipped with three pressure vessels of the same dimensions, $l = 1.0m \times d = 0.167m$. Its weight in air is about 200Kg and the weight-buoyancy force is 35N positive. The VSOR is divided for convenience in two parts: upper and bottom. The upper part of the vehicle contains a layer of PVC tubes for buoyancy properties, a pressure vessel for the electronics and sensors, and the four horizontal thrusters (see Fig. 1). The bottom part of the vehicle consists in two pressure vessels that contain batteries and four vertical thrusters. A small vessel $l = 0.15m \times d = 0.12m$ localised approximately in the vehicle mass center carries an Inertial Measurement Unit. Modular structural components allows that VSOR can be easily reconfigured in agreement with specific tasks. The overall structure of the vehicle is symmetric with respect to both the xz and yz plane.

The VSOR sensor suite is composed by many different sensors. Although not all of them have been used for the experimental trials reported in this paper, we summarise the sensor suite in Table 1.

2.2 Thruster System

The thruster system is composed of eight DC brushless thrusters of Model 1021 of Tecnadyne Inc. Avila [2003] determined that VSOR thruster step response has a time constant of 0.1s. Omitting the dynamics of the VSOR thrusters, the following thruster model is used to calculate the axial force exerted by the propeller:

$$F = aV^2 + bV, \tag{1}$$

where V is the control voltage, which is applied to the thruster servo-amplifiers, a and b are force coefficients which should be identified experimentally using the LS method. The model (1) has been experimentally identified putting the whole actuator in a water tank and measuring the force as a function of a set of input voltages. The tests

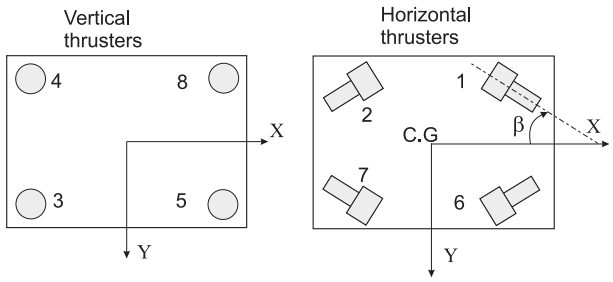

Fig. 2. Sketched top view of the horizontal and vertical thruster configuration.

have been executed in bollard-poll condition. The a and b coefficients values referred to the thruster identified as one are, respectively, $a_1 = 10.84N/V^2$ and $b_1 = -5.019N/V$ for positive thrust.

3. DYNAMIC MODELLING

In this work, we adopt the common practice of approximating the 6-DOF dynamic equation by neglecting off-diagonal entries, coupling terms and tether dynamics, together with the hypothesis of constant added inertia. The simplifications are empirically justified due to slow velocities and relatively small attitude changes which are typical of this class of vehicle. While adopting these hypothesis, one might write a general decoupled 1-DOF equation with the following form:

$$\tau_i(t) = m_i\dot{x}_i(t) + d_{L_i}x_i(t) + d_{Q_i}x_i(t)|x_i(t)| + b_i, \tag{2}$$

$$m_i > 0; \quad d_{L_i}, d_{Q_i} > 0. \tag{3}$$

Where, i represents one particular DOF, $\tau_i(t)$ is the applied force/torque to the vehicle, m_i is the virtual inertia/mass, d_{L_i} is the linear drag coefficient, d_{Q_i} is the quadratic drag coefficient and b_i is the disturbance model. Equation (2) has been used to model the VSOR dynamics in surge ($i = 1$), sway ($i = 2$), heave ($i = 3$), and yaw ($i = 4$). Equation (2) can be written as:

$$\dot{x}_i(t) = \alpha_i x_i(t) + \beta_i x_i(t)|x_i(t)| + \gamma_i\tau_i(t) + \delta_i. \tag{4}$$

The coefficients of (4) are defined in Table 2.

In order to execute experimental trials for the identification of uncoupled hydrodynamic effects and of propeller interactions, the thruster mapping listed in Table 3 has been considered. The horizontal and vertical thrusters are represented by HT_j and VT_j respectively, where the index j relates one particular thruster. Figure 2 shows the allocation of VSOR eight thrusters. For surge motion, front thrusters HT_1 and HT_6 push the vehicle and rear thrusters HT_2 and HT_7 are used for vehicle heading control. In the same manner, for sway motion, front thrusters HT_6 and HT_7 push the vehicle and rear thrusters HT_1 and HT_2 are used for heading control. For heave motion, thrusters VT_3, VT_4, VT_5, and VT_8 push the vehicle and thrusters HT_1 and HT_7 controls the heading.

For surge, sway, yaw but heave motion, thrusters are assumed to work in open water without remarkable interactions with the vehicle hull and other propellers. Therefore, force/torque applied to the vehicle might be calculated as:

Table 1. Sensorial system.

Variable	**Sensor (Manufacturer)**	**Precision**	**Update Rate**	**Output**
Heading	Compass TCM2 (PNI)	$\pm 1^o$	13Hz	Digital
Roll and Pitch	Tilt Series 757 (Applied Geomechanics)	$\pm 2^o$	20Hz	Analog
Depth	Pressure Sensors, MPX5100DP (Motorola)	3.5cm	20Hz	Analog
Yaw Rate	Fiber Optic Gyro, E-Core 2000 (KVH)	Bias $< 2^o$/h	10Hz	Digital
Height	Altimeter, PA200 (Tritech)	1mm	10Hz	Digital
Linear Acceleration	Inertial Measurement Unit, VG700A (Crossbow)	Bias $< \pm 12$mg	100Hz	Digital
Angular Velocity	Inertial Measurement Unit, VG700A (Crossbow)	Bias $< \pm 20^o$/h	100Hz	Digital
Linear velocity: x,y,z	Doppler velocity log (NavQuest 600 Micro)	1mm/s	5Hz	Digital

Table 2. Definition of the VSOR 1-DOF model coefficients.

Coefficient	Physical Definition	Units for Linear Motion	Units for Angular Motion
α_i	$-d_{L_i}/m_i$	[1/s]	[1/s]
β_i	$-d_{Q_i}/m_i$	[1/m]	[rad]
γ_i	$1/m_i$	[1/Kg]	[rad/(Kgm^2)]
δ_i	$-b_i/m_i$	[m/s^2]	[rad/s^2]

Table 3. Thruster system mapping modes.

DOF	Force/torque	Control
Surge	HT_j $j = 1, 6$	HT_j $j = 2, 7$
Sway	HT_j $j = 6, 7$	HT_j $j = 1, 2$
Heave	VT_j $j = 3, 4, 5, 8$	HT_j $j = 1, 7$
Yaw	HT_j $j = 1, 7$	

$$\begin{aligned}
\tau_1 &= \left[(a_1 + a_6)V^2 + (b_1 + b_6)V\right] cos(\beta),\\
\tau_2 &= \left[(a_6 + a_7)V^2 + (b_6 + b_7)V\right] sin(\beta),\\
\tau_3 &= \eta\left[(a_3 + a_4 + a_5 + a_8)V^2 + (b_3 + b_4 + b_5 + b_8)V\right],\\
\tau_4 &= \left[(a_1 + a_7)V^2 + (b_1 + b_7)V\right] R. \qquad (5)
\end{aligned}$$

which is obtained by the use of (1). In the adopted notation, β is the module of the angle between the horizontal thrusters and the vehicle longitudinal axis. For τ_4, R is the moment arm of the respective horizontal trusters. R is measured in relation to the VSOR mass center from a top view. For τ_3, η is the thruster installation coefficient which takes into account the overall reduction in thruster efficiency while applying the desired 1-D force/torque.

4. YAW CONTROL SYSTEM DESIGN

During experimental trials the vehicle heading must be kept constant by the action of a heading autopilot. A conventional proportional-derivative (PD) heading controller based on the vehicle dynamic model, described by (2), has been designed. Neglecting any interaction between the yaw motion and other motions, the dynamics of the yaw motion is of the form:

$$\ddot{\psi}(t) = -\frac{c_1}{I}\dot{\psi}(t) - \frac{c_2}{I}\dot{\psi}(t)|\dot{\psi}(t)| + \frac{1}{I}\phi(t), \qquad (6)$$

where $\psi(t)$, $\dot{\psi}$, and $\ddot{\psi}$ are, respectively, the angular position, velocity, and acceleration; $\phi(t)$ is the external torque applied to the vehicle; c_1 and c_2 are the linear and quadratic rotational drag coefficients, and I is the yaw virtual inertia of the vehicle.

The state error coordinates are defined as:

$$\begin{aligned}
\Delta\psi(t) &= \psi_d(t) - \psi(t),\\
\Delta\dot{\psi}(t) &= \dot{\psi}_d(t) - \dot{\psi}(t),\\
\Delta\ddot{\psi}(t) &= \ddot{\psi}_d(t) - \ddot{\psi}(t), \qquad (7)
\end{aligned}$$

where ψ_d and $\dot{\psi}_d$ are the desired yaw angular position and velocity.

Given a reference angular position ψ_d, the controller must allow null steady-state error. The nonlinear state equation (6) is linearised around $\dot{\psi}_d = 0$, obtaining the following linear model:

$$\Delta\ddot{\psi}(t) = -\frac{c_1}{I}\Delta\dot{\psi}(t) + \frac{1}{I}\phi_\delta(t). \qquad (8)$$

where $\phi_\delta(t)$ is the feedback control action. $\phi_\delta(t)$ is defined as:

$$\phi_\delta(t) = -k_p\Delta\psi(t) - k_d\Delta\dot{\psi}(t), \qquad (9)$$

where k_p and k_d are error feedback gains.

Substituting (9) into (8), the resulting closed loop dynamical system is given by:

$$I\Delta\ddot{\psi}(t) + (c_1 + k_d)\Delta\dot{\psi}(t)| + k_p\Delta\psi(t) = 0 \qquad (10)$$

which is a linear system that is time invariant in the error coordinates.

As defined, c_1, k_p, and k_d are positive constants, therefore the closed loop dynamic system (10) has a globally asymptotically stable equilibrium point at the origin, i.e, $\Delta\psi(t) = \Delta\dot{\psi}(t) = 0$.

The PD controller output given by (9) is updated with a frequency of 13Hz that corresponds to the compass sampling rate.

For the heave motion, the required torque by the controller, Y, which should be applied by thrusters HT_1 and HT_7, in order to correct heading error, is calculated using the following expression:

$$Y = \left[(a_1 + a_7)V^2 + (b_1 + b_7)V\right] cos(\beta)R. \qquad (11)$$

The implementation of the vehicle heading controller considers the solution in each discrete time instant of the following second degree polynomial equation:

$$(a_1 + a_7)V^2 + (b_1 + b_7)V - \frac{Y}{cos(\beta)R} = 0. \qquad (12)$$

The solution of (12) determines the voltage, V, that should be applied to the vehicle thrusters in order to correct heading error. The parameter tuning of the controller has been done experimentally, $k_p = 300$ and $k_d = 150$ has been obtained.

5. PARAMETER IDENTIFICATION METHOD

In this section, the parameter identification method, named integral method, is presented. The method is basically equivalent to the classical least squares algorithm applied to the integral form of the system dynamic equations. We rely on the work of Ridao et al. [2004] but develop expressions for only one DOF.

Equation (4) might be expressed for the i-th DOF in the following form:

$$\dot{x}_i(t) = \phi(x_i(t), \tau_i(t))\theta, \tag{13}$$

$$y_i(t_k) = x_i(t_k) + e_i(t_k), \tag{14}$$

where, $\phi(x_i(t), \tau_i(t))$ is a vector valued function defined by,

$$\phi = [\, x_i(t) \;\; x_i(t)|x_i(t)| \;\; \tau_i(t) \;\; 1 \,], \tag{15}$$

θ is the parameter vector defined by:

$$\theta = [\, \alpha_i \;\; \beta_i \;\; \gamma_i \;\; \delta_i \,]^T, \tag{16}$$

$y_i(t_k)$ is the observable output and $e_i(t_k)$ is the measurement error.

The estimation of the parameter vector θ is equivalent to the minimisation of the scalar cost function given by:

$$J(\theta) = \frac{1}{N}\sum_{k=1}^{N} \epsilon_i^T(t_k) W^{-1}(t_k) \epsilon_i(t_k). \tag{17}$$

The cost function is a weighted sum of squared prediction errors $\epsilon_i(t_k)$, which is defined by:

$$\epsilon_i(t_k) = y_i(t_k) - \hat{y}_i(t_k). \tag{18}$$

The sequence of positive scalars $\left\{W^{-1}(t_k)\right\}_{k=1}^{N}$ are weights related to the reliability of measurements at each time instant. If the measurement noise $e_i(t_k)$ has zero mean, then the expected value of (14) is given by:

$$\hat{y}_i(t_k) = \hat{x}_i(t_k), \tag{19}$$

where $\hat{x}_i(t_k)$ is the estimate of the expected state at time t_k. The minimisation of the cost function given by (17) requires the availability of an estimate of the one-step ahead prediction of the output $\hat{y}(t_k)$. A possible way of obtaining an estimate of $\hat{y}(t_k)$ is described in the following:

At first, consider (13) in two consecutive time instants, subtract them and integrate:

$$x_i(t_k) - x_i(t_{k-1}) = \left[\int_{t_{k-1}}^{t_k} \phi(x_i(s), \tau_i(s))ds\right]\theta. \tag{20}$$

We assume that,

$$x_i(t_{k-1}) = \tilde{y}_i(t_{k-1}), \tag{21}$$

where $\tilde{y}_i(t_{k-1})$ is a filtered version of the output vector $y_i(t_{k-1})$. Therefore, it is possible to write:

$$\hat{x}_i(t_k) = \tilde{y}_i(t_{k-1}) + \boldsymbol{H}_k\theta, \tag{22}$$

where,

$$\boldsymbol{H}_k = \int_{t_{k-1}}^{t_k} \phi(\hat{x}_i(s), \tau_i(s))ds. \tag{23}$$

In this way, it is possible to compute the one-step ahead prediction error of (18) by:

$$\epsilon_i(t_k) = \tilde{y}_i(t_k) - \tilde{y}_i(t_{k-1}) - \boldsymbol{H}_k\theta. \tag{24}$$

Reordering (24), we might write:

$$\tilde{y}_i(t_k) - \tilde{y}_i(t_{k-1}) = \boldsymbol{H}_k\theta + \epsilon_i(t_k). \tag{25}$$

It is possible to equally write:

$$\tilde{x}_i(t_k) - \tilde{x}_i(t_{k-1}) = \boldsymbol{H}_k\theta + \epsilon_i(t_k). \tag{26}$$

Now, writing (26) for $k = 1, \ldots, N$ the following matrix equation is obtained:

$$\boldsymbol{Y} = \boldsymbol{H}\boldsymbol{\theta} + \boldsymbol{\epsilon}. \tag{27}$$

Where:

$$\boldsymbol{Y} = \begin{bmatrix} \tilde{x}_i(t_1) - \tilde{x}_i(t_0) \\ \tilde{x}_i(t_2) - \tilde{x}_i(t_1) \\ \cdots \\ \tilde{x}_i(t_k) - \tilde{x}_i(t_{k-1}) \\ \cdots \\ \tilde{x}_i(t_N) - \tilde{x}_i(t_{N-1}) \end{bmatrix}, \tag{28}$$

$$\boldsymbol{H} = [\, \boldsymbol{H}_1 \;\; \boldsymbol{H}_2 \;\; \boldsymbol{H}_3 \;\; \boldsymbol{H}_4 \,], \tag{29}$$

where,

$$\boldsymbol{H}_1 = \begin{bmatrix} (t_1 - t_0)\tilde{x}_i(t_0) \\ (t_2 - t_1)\tilde{x}_i(t_1) \\ \cdots \\ (t_k - t_{k-1})\tilde{x}_i(t_{k-1}) \\ \cdots \\ (t_N - t_{N-1})\tilde{x}_i(t_{N-1}) \end{bmatrix}, \tag{30}$$

$$\boldsymbol{H}_2 = \begin{bmatrix} (t_1 - t_0)\tilde{x}_i(t_0)|\tilde{x}_i(t_0)| \\ (t_2 - t_1)\tilde{x}_i(t_1)|\tilde{x}_i(t_1)| \\ \cdots \\ (t_k - t_{k-1})\tilde{x}_i(t_{k-1})|\tilde{x}_i(t_{k-1})| \\ \cdots \\ (t_N - t_{N-1})\tilde{x}_i(t_{N-1})|\tilde{x}_i(t_{N-1})| \end{bmatrix}, \tag{31}$$

$$\boldsymbol{H}_3 = \begin{bmatrix} (t_1 - t_0)\tau_i(t_0) \\ (t_2 - t_1)\tau_i(t_1) \\ \cdots \\ (t_k - t_{k-1})\tau_i(t_{k-1}) \\ \cdots \\ (t_N - t_{N-1})\tau_i(t_{N-1}) \end{bmatrix}, \tag{32}$$

$$\boldsymbol{H}_4 = \begin{bmatrix} (t_1 - t_0) \\ (t_2 - t_1) \\ \cdots \\ (t_k - t_{k-1}) \\ \cdots \\ (t_N - t_{N-1}) \end{bmatrix}, \tag{33}$$

and

$$\boldsymbol{\epsilon} = [\, \epsilon_i(t_1) \;\; \epsilon_i(t_2) \;\; \cdots \;\; \epsilon_i(t_N) \,]^T. \tag{34}$$

Equation (27) is linear in the vector of parameters $\boldsymbol{\theta}$, therefore, the parameters might be estimated by the classical Least-Squares algorithm:

$$\boldsymbol{\theta}_{LS} = (\boldsymbol{H}^T\boldsymbol{W}^{-1}\boldsymbol{H})^{-1}\boldsymbol{H}^T\boldsymbol{W}^{-1}\boldsymbol{Y}. \tag{35}$$

where $\boldsymbol{W}^{-1}$ is a diagonal matrix with the principal diagonal given by:

$$\left[\, W^{-1}(t_1) \;\ldots\; W^{-1}(t_k) \;\ldots\; W^{-1}(t_N) \,\right]. \tag{36}$$

6. TEST TANK EXPERIMENTS

Trials have been conducted in the Naval and Oceanic Engineering Department test tank. Free running experiments in surge, sway, heave and yaw motions have been done. Multiple trials in each DOF, one DOF at a time, have been executed with sinusoidal thrust profiles of varying magnitude and frequency. In this work, it is reported only results for yaw motion. The identification experiments have been performed by applying input torque with thruster mapping having unit efficiency, i.e., thrusters HT_1 and HT_7 have been used for positive torque (clockwise movements), see Fig. 2. Thruster have unit efficiency when

Table 4. Sinusoidal voltage profiles applied to thrusters 1 and 7.

Group	Amplitude A (V)	Voltage Offset V_0 (V)	Periods (s)
YAW1	0.8	1.6	2, 4, 8, 16, 24 and 30
YAW2	1.3	2.1	2, 4, 8, 16, 24 and 30
YAW3	1.8	2.6	2, 4, 8, 16, 24 and 30

their produced torque during the experiment is considered to be the same as that produced in test tank bollard-pull conditions.

Three types of experiments named YAW1, YAW2, and YAW3 have been executed and their respective sinusoidal control voltages applied to thrusters are presented in the Table 4. The input torque is calculated according to (5).

6.1 Numerical Results

This section reports numerical results of the experimental parameter identification of the vehicle yaw motion dynamics using the integral method outlined above. An evaluation assessment of the *quality* of parameter estimates are realised using two procedures:

(1) Comparing experimental logged data sets with simulation models based on parameter estimates derived from the same experimental data set, and
(2) comparing the dynamics of a simulation model using other experimental data sets that are different from the one used for parameter estimation.

The integral parameter identification method has been applied to experimental data sets that corresponds to YAW1, YAW2 and YAW3 (see Table 4). Subsequently, numerical simulations have been run using a Fourth Order Runge-Kutta ODE integration algorithm. The simulations have been run using actual logged torque profiles and the simulation system output is yaw angular velocity, ν_{model}, which has been compared to the experimental logged yaw angular velocity $\nu_{measure}$. The adopted error performance measure is the absolute mean error:

$$e = \text{mean}(|\nu_{model} - \nu_{measure}|). \tag{37}$$

The parameter estimates with best performance are listed in Table 5 which corresponds to the experimental data set of YAW2, more specifically, this corresponds with the following voltage profile: amplitude $A = 1.3$V, offset $V_0 = 2.1$V, and Period = 30s .

Fig. 3 illustrates the experimental data set used for the dynamic model identification of the yaw motion. Top plot shows the input torque profile used to excite the vehicle. The middle plot shows the vehicle logged heading with measurements provided by the electronic compass and the bottom plot shows the estimated vehicle yaw rate. The yaw rate has been obtained by numerically differentiating the heading signal and then filtering it with a 2nd order Butterworth low pass filter. Plots of the simulated yaw rate ν_{model}, experimental yaw rate $\nu_{measured}$ and the yaw rate error $\nu_{model} - \nu_{measured}$ are shown in Fig. 4. It shows that the simulated yaw rate, based on the estimated dynamic model, see Table 5, agrees closely with the experimental yaw rate.

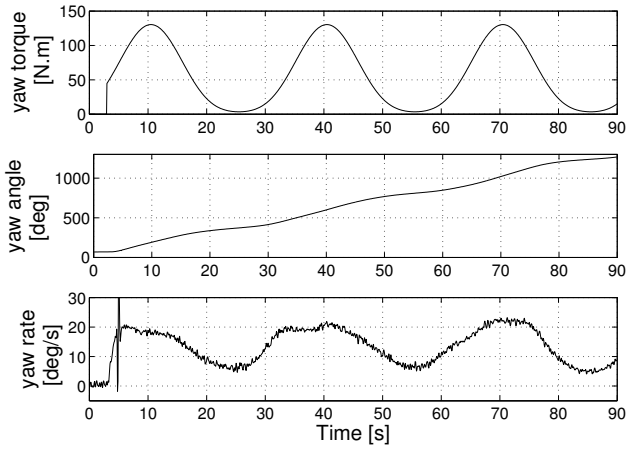

Fig. 3. Experimental data set for the identification of the VSOR yaw dynamic model. Top: Applied nominal torque. Middle: Logged heading with 13Hz sampling rate. Bottom: yaw rate (angular velocity).

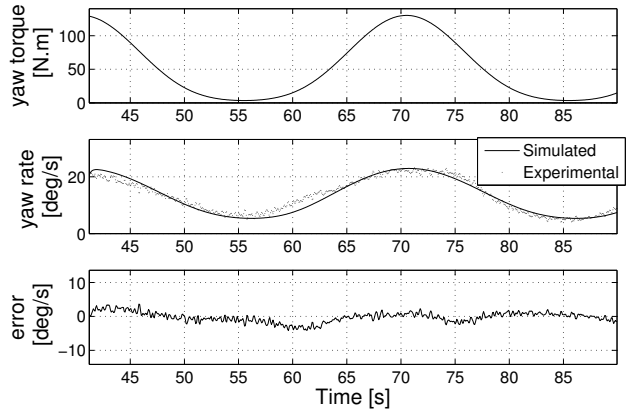

Fig. 4. Comparison of simulation results and experimental data of yaw motion. Top: Applied nominal torque. Middle: yaw rate (angular velocity). Bottom: velocity error.

As parameter estimates are obtained from one experimental data set, it is reasonable to expect that the simulation results will fit closely this particular experimental data set. An important issue which arises in experimental model identification is whether or not the system model with parameters estimated from one particular experimental data set can accurately generalise under different experimental conditions. In this section, numerical simulations have been run on the identified system model using different input torque profiles.

Fig. 5 shows simulation results using different input torque profile. Plot indicates some phase-shift problem.

We have observed that a system model with parameters estimated with half-magnitude torque profiles (YAW2) and larger period of excitation, performed uniformly well - the single model accurately predicts experimentally observed dynamics at all thrust levels (YAW1, YAW2, and YAW3). In contrast, a system model with parameters estimated using low magnitude torque profile have performed poorly - the single model has good performance in predicting

Table 5. VSOR yaw dynamic model: Hydrodynamic parameters.

$\alpha\ [1/s]$	$\beta\ [rad]$	$\gamma\ [rad/(kg.m^2)]$	$\delta\ [rad/s^2]$	Error $e\ [rad/s]$
-0.5478	-4.9945	0.007317	0.068256	0.01555
$d_L\ [kg.m^2/(rad.s)]$	$d_Q\ [kg.m^2]$	$m\ [kg.m^2/rad]$	$b\ [N.m]$	
74.867	682.57	136.66	-9.3282	

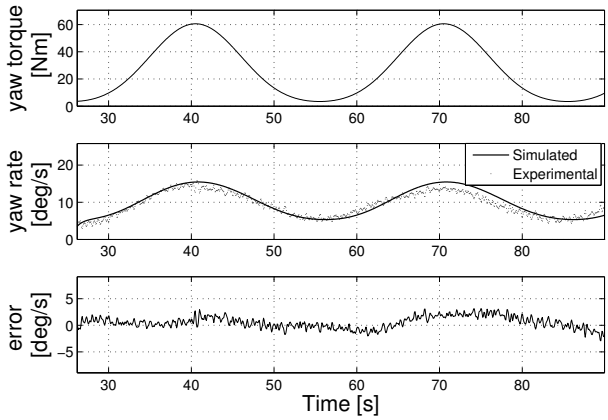

Fig. 5. Comparison of simulation results and experimental data corresponding to YAW1. Sinusoidal voltage profile: Amplitude $A = 0.8$V, Offset $V_0 = 1.6$V and Period = 30s.

experimentally observed dynamics only for thrust profiles similar to the ones that occurred in the data set used for its own parameter estimates. In summary, the system excitation with half-magnitude torque profiles and larger period $= 30s$ is sufficient to provide accurate and fast parameter estimation in the presence of measurement noise and actuator disturbances.

7. DISCUSSIONS

The VSOR virtual inertia m, can be assumed to be equal to the inertia in air m^{air} plus 100% of m^{air} that models the added inertia, see Caccia et al. [2000]. Considering that, $m^{air} = 60\text{Kgm}^2$ (obtained with the AUTOCAD software), then $m = 120\text{Kgm}^2$. This last value is in agreement with the experimental parameter estimate of $m_i = 136.66\text{Kgm}^2$ (see Table 5). Therefore, the parameter estimate for the virtual mass m_i is consistent with our physical understanding of the vehicle design.

It has also been observed that for larger values of amplitude and period of the input torque profile, the vehicle experiences larger variations in position, velocity, and acceleration improving the signal-to-noise ratio of the experimental data and, as a consequence, provides more accurate model parameter estimation.

8. CONCLUSIONS

In this work a methodology for the experimental identification of hydrodynamic parameters of yaw motion dynamics of an open-frame underwater vehicle has been presented. The methodology is based on the utilization of an uncoupled 1-DOF dynamic system equation of an underwater vehicle and the application of the integral method which is the classical least squares algorithm applied to the integral form of the system dynamic equations.

Experimental trials have been performed in a test tank. The effects of different thrust profiles on model parameter identification have been investigated, confirming that, simulation models have better performance when their parameters are estimated with experimental data sets with sinusoidal thrust profiles of relatively larger magnitude and period. When hydrodynamic nonlinear dynamic system models of open-frame underwater vehicles, that might be represented by (4), are properly identified, they exhibit both steady-state and dynamic response that closely agrees with the experimentally observed response over a wide range of operating conditions.

ACKNOWLEDGEMENTS

The authors would like to thank the FINEP for financial support through the CTPetro/ANP program, the CNPq for scholarship and financial support, the FAPESP for scholarship support, the CENPES/PETROBRAS for the logistic support and the Windriver Inc. for the donation of the Vxworks operating system and the Tornado development system.

REFERENCES

Juan Pablo Julca Avila. Hydrodynamic coefficient estimation of a semi-autonomous underwater vehicle (In Portuguese). Master's thesis, Polytechnic School, University of Sao Paulo, 2003.

M. Caccia, G. Indiveri, and G. Veruggio. Modelling and identification of open-frame variable configuration underwater vehicles. *IEEE Journal of Oceanic Engineering*, 25(2):227–240, 2000.

P. Ridao, A. Tiano, A. El Fakid, M. Carreras, and A. Zirilli. On the identification of non-linear models of unmanned underwater vehicles. *Control Engineering Practice*, 12:1483–1499, 2004.

David A. Smallwood and Louis L. Whitcomb. Adaptive identification of dynamically positioned underwater robotic vehicles. *IEEE Transactions on Control Systems Technology*, 11(4):505–515, July 2003.